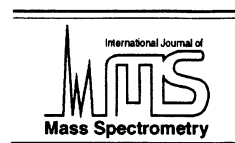




ELSEVIER



International Journal of Mass Spectrometry 178 (1998) 173–186

Motional averaging of ions for control of magnetron motion in Fourier transform ion cyclotron resonance open-geometry trapped-ion cells

Victor H. Vartanian¹, David A. Laude*

Department of Chemistry and Biochemistry, University of Texas at Austin, Austin, TX 78712, USA

Received 20 May 1998; accepted 15 June 1998

Abstract

Open trapped-ion cell geometries have been utilized extensively in external source Fourier transform ion cyclotron resonance (FTICR) applications. A fundamental difference between open and closed cells is that in open cells the radial electric field undergoes a shift in orientation as a function of z displacement. Ions confined near the cell radial centerline in the z center of the cell experience an outward-directed destabilizing field gradient force whereas ions at large axial amplitude encounter an inward-directed stabilizing force. Radial destabilization at the center of the cell is compensated by radial stabilization at increased z amplitude through motional averaging along the z axis. This suggests that conditions can be created in the open cell for which deleterious effects due to magnetron motion can be minimized. This contrasts with the closed cell, for which the radial electric field is outward directed at every point along the z axis. This unique aspect of the open geometry trapped-ion cell is demonstrated to reduce radial drift by control of the axial amplitude of the ion cloud. Suspended trapping and resonance excitation of the trapping motion are used to increase the ion z amplitude. For ions with increased z amplitude, the effective cyclotron frequency (ω_+) approaches the unperturbed cyclotron frequency (ω_c) with virtual elimination of the magnetron frequency (ω_-). This is observed in benzene for which ω_+ is observed only 16 Hz below ω_c . Additionally, resonant excitation at the trapping frequency ($2\omega_t$) was used to increase the axial extent of the ion cloud, raising cyclotron frequency up to 550 Hz. The cyclotron frequency shift also occurs without peak broadening. This radial trajectory stabilizing characteristic of the open cell was maximized using shallow trapping wells in nested traps that yielded cyclotron frequency shifts 300 Hz higher than the unperturbed cyclotron frequency. This is a result of longer ion residence time at the turnaround points in the trapping well (where the inward-directed radial electric field is greatest in magnitude), increased axial extent of the ion cloud due to ion Coulomb repulsion, and the shallower trapping well. The presence of large numbers of charges (electrons, negative ions) in the outer trapping wells of polarity opposite the positive ions in the central trapping well may compensate for the depression of cyclotron frequency due to space charge. (Int J Mass Spectrom 178 (1998) 173–186) © 1998 Elsevier Science B.V.

Keywords: Fourier transform ion cyclotron resonance; Open cell; Magnetron motion; Radial electric field

1. Introduction

Fourier transform ion cyclotron resonance mass spectrometry (FTICR/MS) obtains the mass-to-charge

ratio of ions by the characteristic cyclotron frequency exhibited in a homogeneous magnetic field [1]. Ion confinement in three dimensions is achieved radially by the magnetic field Lorentz force and axially by imposition of an electrostatic field parallel to the magnetic field axis (by convention, a coordinate system is designated in which ions are constrained radially in the xy dimension and axially in the z dimension).

* Corresponding author.

¹ Present address: Motorola Semiconductor Product Sector, Advanced Product Research and Development Laboratory, 3501 Ed Bluestein Blvd., Mail Drop K10, Austin, TX 78721.

In an ideal cell having endcap electrodes of infinite extent, the magnetic and electrostatic forces produce two modes of motion, the radial cyclotron motion and the axial trapping motion. As a result of trap electrode truncation, an incident $\mathbf{E} \times \mathbf{B}$ field creates an additional radial force from the radial electric field (E_r) that induces drift motion around equipotential lines, resulting in magnetron motion [2]. This destabilizing motion partially cancels the effective Lorentz force, limits the critical mass that can be stored in the trap [3], and causes ion loss and reduced sensitivity. The magnitude of the cyclotron frequency reduction is a measure of the magnetron frequency because energy is conserved in the radial modes of motion [4]. The reduced cyclotron frequency (ω_+) is related to the unperturbed cyclotron frequency (ω_c) and the magnetron frequency (ω_-) according to the following equation [5]:

$$(\omega_c) = (\omega_+) + (\omega_-) \quad (1)$$

In all closed cells, the radial electric field is outward directed at every position along the z axis. Ions undergo a field gradient force directed away from the radial centerline of the trap at every point along the z axis. However, in open-ended trapped-ion cells the radial electric field is outward directed at the center of the cell but changes orientation and becomes inward-directed at increased axial displacement in the proximity of the endcap electrodes. The average radial electric field an ion encounters as it oscillates in the trapping well then depends on its axial amplitude. Ion axial amplitude in an open trapped-ion cell can be manipulated so that motional averaging of the axially dependent radial electric field results in radially stabilized ion motion [6] determined by cyclotron frequency detected close to the unperturbed frequency. In experiments designed to control the z axis amplitude of a resident ion population in an open cell, cyclotron frequency shifts as a function of axial amplitude in the position dependent radial electric field.

2. Theory

2.1. Closed and open cell radial electric fields: effect on magnetron motion

Our interest in this work is the evaluation of the open-ended trapped-ion cell radial electric field and characteristic ion motion compared to the closed geometry trapped-ion cell. Shown in Fig. 1(a) is the SIMION [7] plot of the radial electric field at a 1 mm radial displacement from the cell centerline as a function of axial position for a closed elongated trapped-ion cell of aspect ratio 2. Cells having closed endcaps produce a radial electric field that is outward directed at every position along the z axis, with increasing magnitude as a function of radial position.

The open ended trapped-ion cell was first used by Byrne and Farago to study polarization transfer from atomic beams [8], by Malmberg and de Grassie to study electron plasmas [9–11], and by Gabrielse and co-workers for making high precision trapping frequency measurements of the electron and antiproton [12–18]. In the initial open cell work introduced to FTICR by Beu and Laude [19], it was recognized that a shift in the radial electric field orientation at increased z amplitude should result in reduced frequency shift compared to a closed cell of the same aspect ratio. The reversal of the radial electric field is shown in Fig. 1(b) for the standard open trapped-ion cell of aspect ratio 2, and is a feature common to all open trapped-ion cells. An open cell having a single annular trap electrode in the center of the trapping region shown in Fig. 1(c) also exhibits a shift in radial electric field orientation at increased z amplitude. In principle, there should be several interesting experimental manifestations of this effect. As ions oscillate in the trapping well, the *average* radial electric field encountered is reduced due to the effect of the inward-directed radial electric field compared to a cell having only an outward-directed field. Ions with significant z amplitude should exhibit a motion-averaged effective cyclotron frequency that approaches ω_c as the inward-directed radial electric field reduces the effect of the outward-directed radial electric field on cyclotron frequency, resulting in

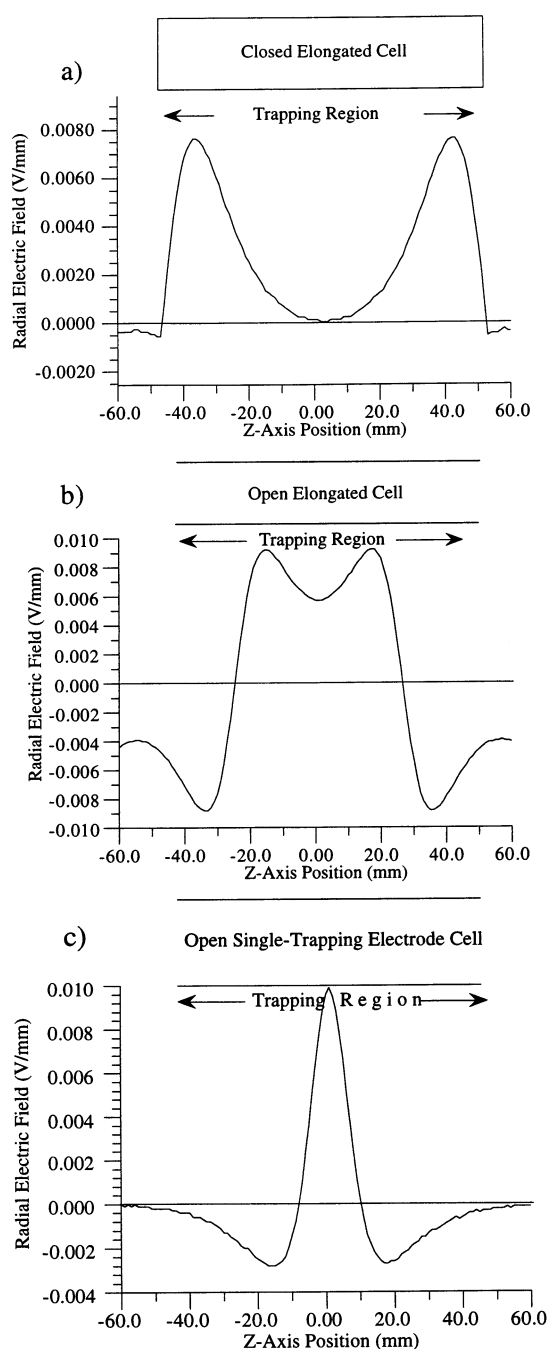


Fig. 1. (a) Closed elongated cell radial electric field at a 1 mm radial displacement from the cell centerline as a function of z -axis position. The direction of the radial electric field is outward (positive) at every position along the z axis. (b) Open elongated cell radial electric field at a 1 mm radial displacement from the cell centerline as a function of z -axis position. The direction of the

reduced magnetron motion as ions are maintained along the z axis. Such a phenomenon would be applicable to experiments in which the primary limitation is radial ion loss [20].

In a closed trapped-ion cell, the axial electric field that traps ions simultaneously produces a repulsive force directed in the radial direction. Thus, Earnshaw's theorem states that a three-dimensional local potential minimum, or potential well, cannot be formed in space by static potentials alone [21]. Magnetic fields in addition to dc fields (as in Penning traps) or rf fields (as in Paul traps) must be used to trap ions in three dimensions. In the case of a Penning trap, the electrostatic trapping field enters the trap axially and exits radially, producing E_r . The immediate impression of an inward-directed radial electric field in a Penning trap using only electrostatic potentials is that it is in violation of Earnshaw's theorem because simultaneous axial and radial restoring forces suggest a three-dimensional well. However, the inward-directed radial electric field occurs only at extended z amplitude, while the outward-directed radial electric field occurs at the center of the cell, so that along the z axis there is no net inward-directed radial electric field. Ions cannot be trapped indefinitely in this part of the field because the axial restoring force directs them to the center of the cell where the field is outward directed. The effect is periodic and relies on motional averaging with ions possessing sufficient axial kinetic energy to penetrate the region of the cell where the radial electric field is outward directed. However, ions spend a substantial fraction of their trapping oscillation time near the turnaround points where the radial field is inward directed because of reduced translational velocity at the peak of the potential well. Thus, ions can be radially stabilized through their axial motion. Only an open geometry trap with endcap electrodes positioned

radial electric field is outward at the center of the cell but becomes negative (inward) at increased z -axis displacement. (c) Single annular trap electrode cell radial electric field at a 1 mm radial displacement from the cell centerline as a function of z -axis position also indicating a radial electric field shift at increased z -axis displacement.

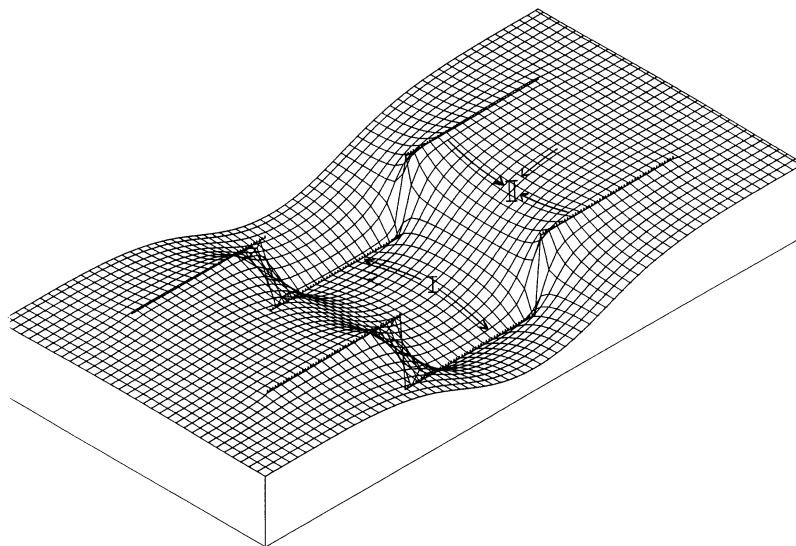


Fig. 2. Three-dimensional SIMION contour plot for a conventional two-endcap electrode open cell depicting radial electric field vectors. The direction of the radial electric field is shown at two locations along the z axis of the trapping well with arrows depicting the outward-directed force at the cell center (I) and the inward-directed force near the potential maxima in the vicinity of the endcap electrodes (II). The axially inward-directed arrow represents the trapping force.

parallel to the axis of ion motion could exhibit a variation in the radial electric field coincident with the ion trapping motion. The effect of ion axial oscillation along a set of endcap electrodes having radial electric field of varying orientation is analogous to alternating the potential on the endcap electrodes.

Fig. 2 provides a three-dimensional SIMION isopotential contour representation of the potential well in a conventional two-trap electrode open cell that better illustrates the axial dependence of the radial electric field. As in closed trapped-ion cells, a potential maximum at the center of the cell ($x, y = 0$) decreases to zero potential at the grounded excitation/detection electrodes, and an outward-directed radial electric field is observed at point I. This field is the source of the unstable magnetron trajectory. However, along the z axis of all open cells adjacent to the endcap electrodes is a region in which there is not only an axial restoring force directed toward the center ($z = 0$) of the cell but also a radial restoring force that is directed toward the centerline of the cell at point II. The result is an inward-directed radial shift in ion trajectory for ions located at axial displace-

ments approaching the potential energy maxima in the trapping well. Ions travel radially away from and, subsequently, toward the cell centerline as they oscillate within the trapping well, thus encountering a motional-averaged radial electric field that is a function of axial oscillation amplitude. The difference of the unperturbed cyclotron frequency and the reduced cyclotron frequency then becomes a measure of the average radial electric field encountered in the trapping well, which is also a function of the axial oscillation amplitude.

The average radial electric field at 1 mm radial displacement from the cell centerline encountered by ions as they traverse the trapping well is shown in Fig. 3. The radial electric field is averaged over 1 mm increments, showing that for the closed cell, ions undergoing large amplitude trapping motion encounter a significant outward-directed radial force that results in their rapid radial drift from the cell, whereas ions confined near the center of the cell undergo minimal radial drift. Thus, collisionally damping ions at increased pressure is advantageous in closed cells for maximal resolution and signal detection intensity.

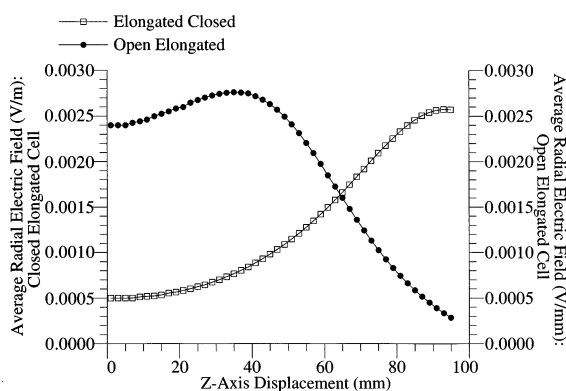


Fig. 3. Radial electric field at 1 mm radial displacement from the centerline of the cell averaged over one trapping period as a function of axial displacement calculated as the summed average at all intermediate positions for closed (open square) and open (filled circle) elongated cells. The average radial electric field is determined by the summation of the radial electric field at every 1 mm axial increment divided by the total axial displacement in millimeters.

For the open cell, ions undergoing large amplitude trapping motion encounter a substantial inward-directed force as they approach the maximum in the trapping potential near the well perimeter. Reduced collisional damping at lower pressure can increase cell residence time. Lower pressure is also commensurate with increased transient lifetime. Thus, the average radial electric field at large z amplitudes in the open cell approaches zero and approximates the average radial electric field at low axial amplitude in the closed elongated cell without collisional damping. The effect of frequency excitation sweeps near the ion trapping frequency would also be less critical in promoting radial ion loss in open cells.

2.2. Temporal versus spatial electric field ion trajectory stabilization

The existence of a radial electric field that radially refocuses ions to the center of the cell can be compared to the creation of a time-averaged “pseudopotential” well in the rf quadrupole ion (Paul) trap. In the quadrupole ion trap, time variation in the potential on the ring electrode creates a potential well in which ions are simultaneously stable in two dimen-

sions but unstable in the other. By rapidly alternating the applied potential, the radial electric field averages to zero; otherwise, ions would eventually be lost from the trap [22]. It is this ability of Paul traps to confine both axial and radial trajectories using only electric fields that enables trapping in three dimensions without radial confinement by a magnetic field as with Penning traps. Ions remain in stable trajectories near the center of the trap because of the effect of the *time-varying* fields.

In an open cell, ions are alternately trapped in an axial well and then in a radial well, although not at the center of the cell simultaneously, but as ions oscillate along the z axis. In the ion frame of reference the trapping field appears to be time varying, whereas in the trap frame of reference it appears to be space varying. Ions remain along the centerline of the cell due to motional averaging of the space-varying radial electric field, analogous to the time-averaged pseudopotential created in the quadrupole ion trap. As long as ions are allowed to oscillate throughout these regions, motional averaging inhibits an increase in magnetron radius. Motional stabilization in a position-varying radial electric field has also been shown to be effective for transporting ions into a trapped-ion cell through a stacked-ring ion guide by altering the sign of the potential on individual electrode segments of an electrostatic lens array. Ions are maintained in a static “pseudopotential” in the center of the guide where the field is weakest [23].

The time-dependent analog of this experiment is the Penning trap operated as a combined trap with magnetic and rf electric fields [24–27]. The unperturbed cyclotron frequency may be detected because magnetron motion is not required to have a reversed energy spectrum. Magnetron motion can cool to the center of the cell by judicious selection of the rf-drive frequency [28]. Similarly, Gorshkov et al. designed a trap for simultaneous confinement of positive and negative ions operating on the principle of dynamically altering the sign of the potentials on the endcap electrodes [29]. This trap also exhibits no cyclotron frequency shift because the sinusoidal trapping field produces no net radial electric field.

2.3. Coulomb models describing peak-shifting and peak-broadening in FTICR

In a perfectly quadrupolar potential well, the radial electric field is independent of axial position so that no position-dependent variation in cyclotron frequency occurs. However, all unsegmented trapped-ion cells exhibit variation of the radial electric field as a function of ion axial position due to endcap electrode truncation where a concave axial electric potential results in a coincident convex radial potential. Peak broadening occurs either as a result of homogeneous relaxation with limited transient lifetime, or due to inhomogeneous relaxation of the ion cloud resulting from variation in the radial electric field as a function of z -axis amplitude or radius. Any change in the *average* radial electric field during detection is a source of inhomogeneous relaxation in the time domain and peak broadening in the frequency domain. Space charge effects also contribute to peak broadening by spreading out the ion cloud over a larger volume in which electric field inhomogeneities are increased, also resulting in cyclotron frequency broadening.

Ions formed within a trapped-ion cell having a distribution of axial positions (such as with electron ionization) or injected into a cell having varying axial amplitudes (such as with externally generated laser desorption) collectively encounter varying average radial electric fields. The ion ensemble would therefore be expected to exhibit peak broadening as a result of axial oscillation of varied amplitudes in the potential well. However, even under experimental conditions most likely to exhibit this type of phenomenon, no peak broadening is observed. For example, when detection immediately follows electron ionization at low pressure, narrow, symmetrical peak shapes are generated. Motional averaging of the radial electric field has been used to explain the lack of peak broadening. Because there is no change in the average radial electric field encountered by all the ions, there is no peak broadening [30]. However, this applies only if the trapping frequency is much greater than the axially dependent variation in the cyclotron frequency ($\omega_z \gg \Delta\omega_c$).

According to the charged-line model [31], because the trapping frequency is usually much greater than the magnetron frequency, motional averaging of the radial electric field during z -axis oscillation yields an average radial electric field which, although shifting cyclotron frequency to lower frequency, also does not generate peak broadening. This is analogous to radial magnetic field inhomogeneity [32], which is motionally averaged during ion cyclotron motion, but does not result in peak broadening [33–36]. For a typical detection period of 10–20 ms, ions oscillate in the trapping well several hundred times and the axial position-dependent radial electric field averages to a single value. As long as minimal axial amplitude variation or radial dispersion occur during the observation time, peak broadening is not observed even though ions encounter variation in the axially dependent radial electric field. If variation occurs in the z amplitude due to collisional damping of the axial motion or in the radial amplitude due to growth in the magnetron radius during the detection process, peak broadening results.

From a practical perspective, this source of peak broadening can be made inconsequential in a typical FTICR experiment. The time scale for ion detection is small compared with the time required to substantially cool the ion z -axis amplitude or for magnetron destabilization to occur, especially in the low pressures typically encountered in FTICR. If long detection times are desired for high mass resolving power, peak broadening is a concern because the observation time may be sufficiently long to permit ions to experience shifts in the radial electric field. The likelihood of shifts in axial amplitude are minimized by implementing the collisional cooling event prior to the detection event and maintaining the lowest possible pressure during detection to reduce collisional damping, usually by pulsing in a collision gas and pumping it away prior to detection.

3. Experimental

All experiments were performed with a single annular trap electrode open cell [37] and a nested

trapped-ion cell [38–41] having four collinear endcap electrodes within a Finnigan FTMS 2000 mass spectrometer (Madison, WI) including a 3.0068(6) T (mass calibration data obtained with 1.0 Hz uncertainty), 150 mm warm-bore superconducting magnet, and 1280 data station executing FTMS software version 6.0.1. The single annular trap electrode cell is 50 mm in diameter and 75 mm in axial dimension. The trapping ring is 3 mm wide and 1 mm thick and is suspended 1 mm above the excitation/detection electrodes using Teflon spacers. By applying a voltage to the ring of opposite bias to the ions, a potential well is formed in the center of the trap which approaches 0 V at the cell boundaries. Additionally, a 25 mm diameter nested, open trapped-ion cell with four trap electrode segments was used to study the effect of various trap voltage combinations on cyclotron frequency. The cell was constructed of 0.76 mm (0.030 in.) thick OFHC copper with the excitation/detection region 23 mm long, the endcap electrodes 17 mm long, and the compensation electrodes 4 mm long with 2 mm air gaps separating all electrodes.

Benzene was introduced at a static pressure through a precision leak valve (Varian Model 951-5106, Lexington, MA) and ionized with a 60 eV, 5 μ A electron beam for 5 ms. Cyclotron frequency was measured as a function of delay time to evaluate the effect of the radial electric field on peak shapes.

The experimental sequence used to obtain the suspended trapping data is comprised of the events Q1, Q2, DQ, BM, D1, S1, D2, S2, D3, S3, EX, DZ, RC. The sequence events Q1 and Q2 are 100 μ s quenches to purge charged particles out of the cell, DQ is a 100 μ s quench delay, and BM is a beam event. The delay events, D1, D2, and D3 are variable time delays in which ions are allowed to damp to the center of the cell ($z = 0$). The suspended trapping events S1, S2, and S3 are each 100 μ s during which the trap voltage is at ground potential. On-resonance excitation at $78 V_{p-p}$ is performed for 100 μ s during EX, DZ is a z -cooling delay, and RC is the signal acquisition event obtained in direct mode over a 2.667 MHz bandwidth, with 16 000 datapoints padded with another 16 000 zeroes followed by sinebell apodization and Fourier transformation.

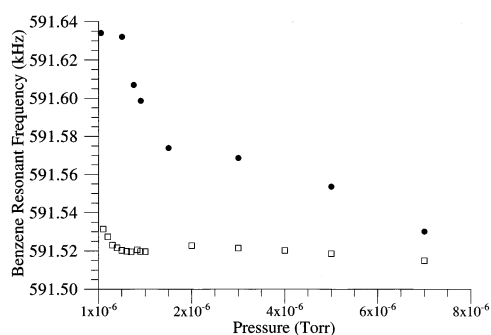


Fig. 4. Dependence of benzene molecular ion cyclotron frequency on neutral pressure with a 5 ms axial cooling delay for a closed cubic (open square) and open single trap electrode (filled circle) cell.

4. Results and discussion

4.1. Cyclotron frequency variation as a function of axial displacement by collisional damping in the open cell radial electric field

Initial experiments to determine the effect of changes in ion cloud axial extent on the detected cyclotron frequency spectral peak position and width were performed at low pressure using ions formed by electron ionization. Increased z -axis amplitude was produced by suspended trapping [42,43] so that the effective cyclotron frequency approached the unperturbed frequency as the ion cloud spent a greater fraction of the z -oscillation time near the perimeter of the cell where it would experience the inward-directed radial electric field. Alternately, collisional cooling of the ions to decrease the axial amplitude of the ion cloud provided a corresponding reduction in the collective cyclotron frequency because ions primarily encountered the effects of the outward-directed radial electric field at the center of the cell.

To illustrate the effects of pressure (corrected) on axial amplitudes in closed and open cells, comparison plots of benzene molecular ion cyclotron frequency as a function of static benzene neutral pressure are shown in Fig. 4 with a 5 ms axial cooling delay. The ionization duration was 5 ms for both cells, with a single-frequency on-resonance excitation duration of 100 μ s at $78 V_{p-p}$. For the cubic cell, cyclotron

frequency decreases as ion number increases with pressure as a result of space charge [44]. At low pressure in the cubic cell, the cyclotron frequency of 591.531 kHz is 87 Hz below the unperturbed cyclotron frequency of 591.618 kHz based on a magnetic field strength of 3.0068(6) T. However, at low pressure in the single-trap electrode cell, cyclotron frequency is 591.634 kHz, 16 Hz above the unperturbed cyclotron frequency. As pressure increases from 1.0×10^{-6} Torr to 7.0×10^{-6} Torr, cyclotron frequency decreases much more rapidly in the single-trap electrode cell than it should because of the effect of increased space charge alone. In this case, as z -axis amplitude decreases with collisional damping, cyclotron frequency approaches the value predicted for ions cooled to the center of an open cell. When ions are cooled to the center of the single-trap electrode open cell, the characteristic linear relationship between frequency shift and applied trap potential is observed [45].

The same kind of dependence of cyclotron frequency on pressure, apart from the effect of space charge, is not observed in closed cells for which there is no inward-directed radial electric field at increased z amplitude to compensate for the effect of the outward-directed radial electric field at the center of the cell. Cooling delays prior to detection result in peak narrowing as ions are located in a volume of reduced electric field inhomogeneity. However, frequency shifts are not observed (unless the ion population changes), apart from the downward frequency shift as a result of greater coulomb repulsion as ions collapse to the center of the cell. Ions having large initial z amplitude in a closed cell should exhibit a modest increase in cyclotron frequency as they cool to the center of the cell where the magnitude of the outward-directed radial electric field is reduced but increased space charge offsets the effect. A slight frequency increase is exhibited in Fig. 4 at 2×10^{-6} Torr in the closed cell as the ion cloud is cooled to the center of the cell, possibly as a result of ion loss. However, the increased space-charge density produced by more ions at higher pressure partially offsets the effect.

In order to manipulate z amplitude of the ion

population, suspended trapping and axial excitation were performed in a single-trap electrode open cell. These experiments verified that an inward-directed radial field at increased amplitude reduces the average radial electric field experienced by ions, seen as an increase in cyclotron frequency and reduction in magnetron motion.

4.2. Manipulation of ion z -axis amplitude by suspended trapping

A series of frequency shift profiles for ions formed in a single trap electrode open cell and allowed to axially cool is shown in Fig. 5(a)–(c). For three trap potentials (-3 , -5 , and -8 V), the effective cyclotron frequency was detected as a function of cooling delay time. Following each delay, a $100 \mu\text{s}$ suspended trapping event was implemented in which the trap electrode was grounded such that the z amplitude of the ions increased as a result of coulombic repulsion. Trap potential was then reinstated prior to detection. As collisional cooling time increased, ions relaxed to the center of the cell where they encountered the outward-directed radial electric field and the cyclotron frequency decreased. The final cyclotron frequency observed also decreases at higher trap potentials. Because ions underwent large z amplitudes immediately after suspended trapping, a frequency of 591.607 kHz approached the unperturbed cyclotron frequency of 591.618 kHz ($\Delta\omega = -11$ Hz). The rate of cyclotron frequency decrease as a function of trap potential is seen as increasingly steeper curves at -5 and -8 V. Increasing the trap potential results in a more rapid collapse of ions to the center of the cell because of the greater slope in the potential well.

As a more stringent test to verify that the observed frequency shift is a function of axial position only, peak position was measured as a function of axial cooling delay at constant trap potential following three consecutive suspended trapping and cooling events for the same ion population. Shown in Fig. 6 are frequency shift plots for three consecutive $100 \mu\text{s}$ suspended trapping events, each followed by 5 s axial cooling delays in the single trap electrode open cell at a constant trap potential of -2 V. With each sus-

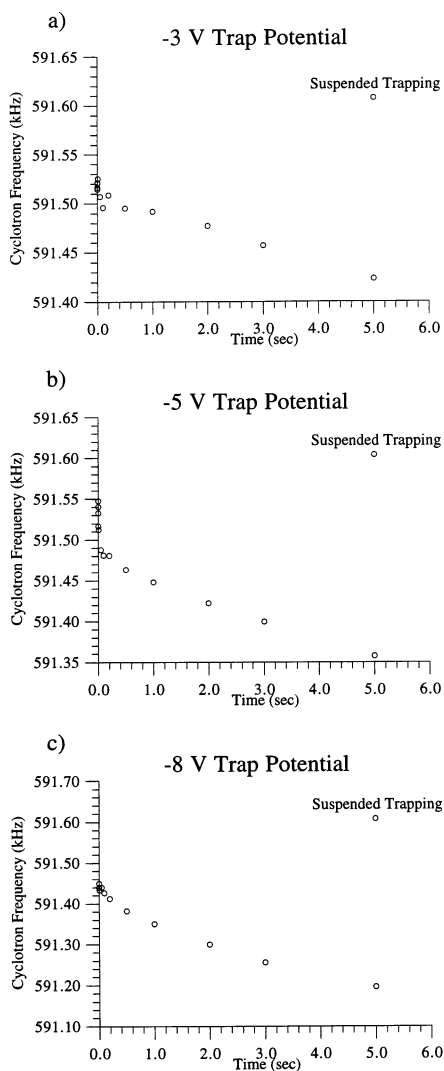


Fig. 5. Cyclotron frequency is plotted as a function of collisional damping delay time followed by a suspended trapping event at three different trap potentials in a single trap electrode open cell: (a) -3 V; (b) -5 V; and (c) -8 V.

pended trapping event, frequency increased close to the unperturbed cyclotron frequency (591.618 kHz), even extending slightly beyond (591.625 kHz). The data provide evidence that at increased z amplitudes in open trapped-ion cells, the ion population encountered a significant radial restoring force that results in a reduction of the magnetron energy observed as an increase in the cyclotron frequency. Even though the

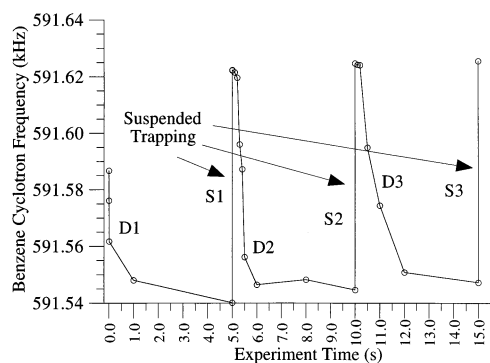


Fig. 6. Plot of benzene cyclotron frequency for a series of three cooling cycles followed by suspended trapping events at a constant trap potential of -2 V as a function of time. Each data point represents a collection of ions that have undergone all the preceding events in the sequence.

ion cloud underwent repeated modulation of its axial amplitude, coherence was still maintained and peak broadening did not occur. Ion loss is apparent by the gradual increase in cyclotron frequency following each suspended trapping event as the charge density in the ion cloud is reduced.

4.3. Direct excitation of the trapping motion

The disadvantage of suspended trapping is axial ion loss during the $100 \mu\text{s}$ suspension of the trapping field (the minimum event time in the FTMS 6.0 system software). As an alternative, resonant excitation at the trapping frequency ($2\omega_z$) can be used to axially disperse the ion cloud to increase cyclotron frequency up to 550 Hz. The result of increasing the axial extent of the ion cloud by direct excitation of the trapping motion is shown in Fig. 7. After the ion cloud is cooled to the center of the cell, excitation at $2\omega_z$ [$\omega_z \approx 8$ kHz] at 16 kHz for $100 \mu\text{s}$ at various excitation levels (11, 9, 7, and no axial excitation) to increase the axial extent of the ion cloud allows ion penetration into the regions of radial stability. As the excitation power is reduced, the axial amplitude of the ion cloud is reduced and ions at lower frequency located closer to the center of the cell increase in relative abundance. Precise control of the ion cloud axial amplitude during excitation is difficult because axial ejection may result

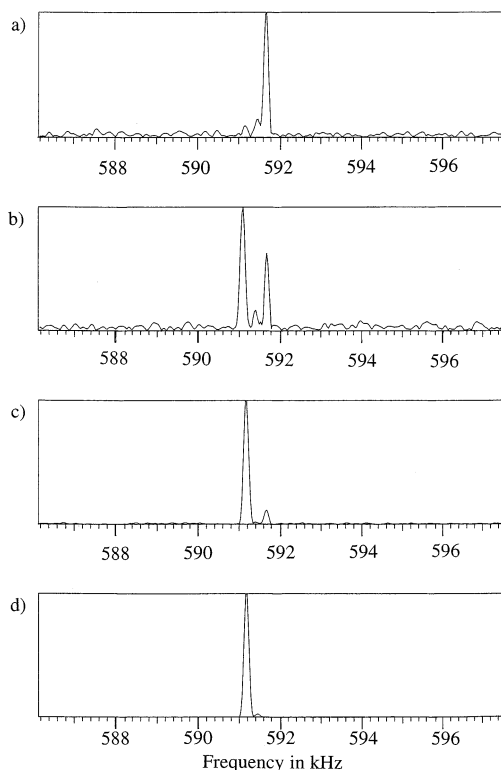


Fig. 7. Excitation of benzene molecular ions at $2\omega_c$ (16 kHz) for $100 \mu\text{s}$ at various excitation levels: (a) $11 V_{p-p}$; (b) $9 V_{p-p}$; (c) $7 V_{p-p}$; (d) no axial excitation, showing increased cyclotron frequency with excitation power.

in a loss of nearly 80% of the ion population. If lower excitation energy or off-resonance axial excitation is applied, cyclotron frequency increases only slightly (about 100 Hz) indicating that the ion cloud does not penetrate sufficiently far into the regions of the inward-directed radial electric field. The persistence of ion packet coherence suggests that the ion packet is not encountering significant variation in the radial electric field during detection.

4.4. Other open cell geometries

An open cell having four endcap electrodes offers considerable experimental flexibility. By applying the same bias to the four endcap electrodes, the cell functions as a conventional open cell. By applying one bias to the inner set of endcap electrodes while a

bias of opposite polarity is applied to the outer set for the simultaneous trapping of positive and negative ions, the cell may function as a nested trap (a potential well of one bias formed within another) [38]. The nested trap has been suggested as a means to produce antihydrogen by passing antiprotons from an accelerator through a trapped cloud of cooled positrons [46]. In addition, the cell may be operated as a compensated trap, with the voltage on the inner traps adjusted to reduce the radial electric field at the center of the cell originating from the outer traps [47]. The reduction in radial electric field at the trap center to near zero is analogous to the screened cell introduced by Wang and Marshall [48].

The nested trap also offers an opportunity to study ion behavior in various radial electric field environments by applying different voltages to each set of endcap electrodes. For example, in a nested trap having the outer endcap electrodes biased to $-6 V$ and the inner endcap electrodes biased to $+3.5 V$, the effective potential well for positive ions in the center of the cell is very shallow because of the superposition of the two opposing electric fields. A shallow potential well results in positive ions spending a greater fraction of their time at the well perimeter rather than at the center of the cell. The radial electric field at increased z -axis amplitude also becomes increasingly inward directed because of the effect of the negative bias from the outer endcap electrodes. In such an arrangement, ions trapped in the central well exhibit increased cyclotron frequency compared to a cell with one set of trap electrode biases.

In open cells, ions may spend a greater fraction of their oscillation time in the regions of the cell where the radial electric field works in concert with the Lorentz force, which consequently results in an effective cyclotron frequency that can exceed ω_c . This unique feature of open cells may be exploited to overcome the destabilizing outward radial drift of ions and increase ion lifetime in the cell. For example, if the ion axial amplitude can be made to increase before each remeasurement cycle, the open cell may also be used to reduce the collision-induced outward radial drift of ions, allowing ions to be refocused back to the center of the cell. Because the primary limitation of

the remeasurement experiment [49–51] is ion loss promoted by the radial electric field [20], the result is an ability to perform remeasurement on low mass ions [6] that are much more susceptible to radial scattering at high pressure [52].

4.5. Effect of nested open cell space charge on cyclotron frequency

In the nested open cell with specific bias combinations applied to the endcap electrodes, cyclotron frequencies have been observed that surpass the calibrated unperturbed cyclotron frequency by several hundred Hertz, with the magnitude of the frequency shift being a function of ion number. This is in contrast to observations in conventional closed or open two-trap electrode cells. For example, Fig. 8(a) is a plot of cyclotron frequency versus neutral benzene pressure from 1×10^{-7} to 1.5×10^{-5} Torr with no cooling delay prior to excitation, indicating that cyclotron frequency increases linearly with pressure. In the open cell, as the number of ions increases, coulomb repulsion of ions along the z axis increases the z extent of the ions. Ions increasingly encounter the inward-directed radial electric field of the negatively biased endcap electrodes at increased z amplitude. As ion number increases and coulomb repulsion increases the axial displacement of the ion cloud, ions remain in the inward-directed radial electric field for a greater fraction of the trapping oscillation period, resulting in an increase in cyclotron frequency. Similar plots of cyclotron frequency versus beam duration and emission current are shown in Fig. 8(b) and (c).

A coulombic effect due to the presence of negative charges in the outer trapping wells may also partially explain the higher cyclotron frequency. Simultaneous storage of positive and negative ions in Paul traps has been performed to improve peak shape and mass accuracy by reducing the space charge of the positive ions [53] and is the basis for trapping large numbers of ions in electron beams for successive ionization to form highly charged ions in an electron beam ion trap (EBIT) [54–56]. Cyclotron frequency increases as the number of negative ions or electrons trapped in the outer trapping wells increases.

To determine the effect of the duration of collisional damping of axial motion on elevated cyclotron frequencies, a plot of cyclotron frequency for benzene as a function of cooling duration is shown in Fig. 8(d) in the nested open cell with -6 V applied to the outer endcap electrodes and $+3.5$ V applied to the inner endcap electrodes. Cyclotron frequency rapidly decreases and levels off as the ion cloud collapses to the center of the cell.

For comparison purposes, Fig. 8(e) illustrates the typical behavior of closed cubic cell cyclotron frequency as a function of beam duration. As the number of ions increases, cyclotron frequency decreases approximately linearly as a function of the radial electric field produced by the ion cloud space charge. This is in contrast to data shown in Fig. 8(b) for the open cell.

5. Conclusions

In open cells the radial electric field undergoes a shift in orientation as a function of axial displacement. Ions confined near the cell radial centerline in the z center of the cell experience an outward-directed destabilizing force whereas ions at large axial amplitude encounter an inward-stabilizing force in contrast to closed cells, in which the radial electric field is outward directed at every point along the z axis. The destabilizing effect of the outward-directed radial electric field in the center of the trap that induces magnetron motion can be compensated by the stabilizing effect of the inward-directed radial field at increased ion axial amplitude. This effect is reflected in the cyclotron frequency as a function of ion cloud axial amplitude. Suspended trapping and resonance excitation of the trapping motion result in increased z amplitude, whereas motional averaging of the ion in the radial electric field along the cell centerline results in increased effective cyclotron frequency approaching the unperturbed cyclotron frequency. Ions also spend a greater fraction of the trapping oscillation time at the turnaround points in the trapping well where their translational velocity is lowest. Reduced pressure reduces axial cooling and allows ions to spend a greater amount of time in the radially stabi-

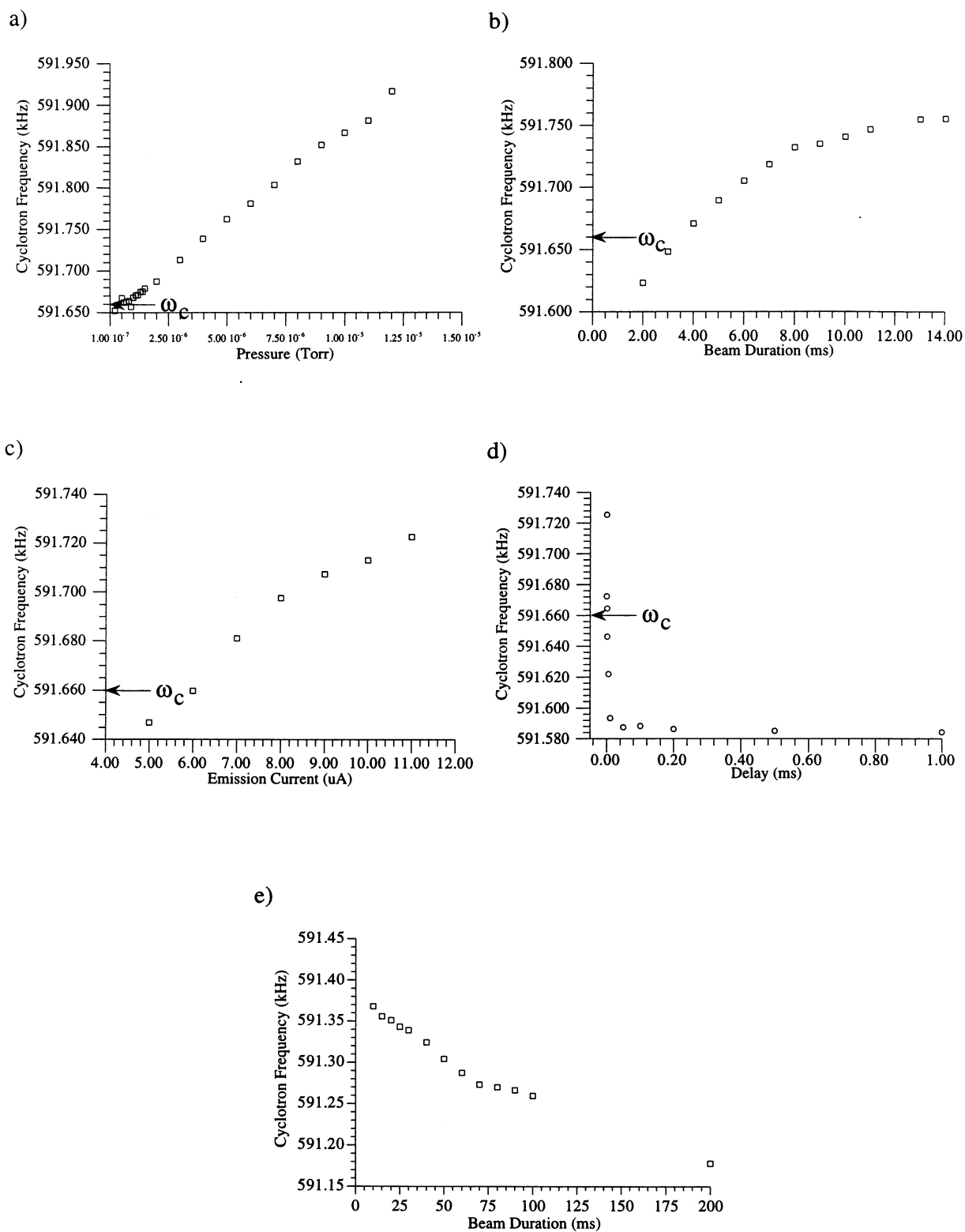


Fig. 8 (caption on facing page)

Fig. 8. (a) Benzene cyclotron frequency vs. pressure in the nested open cell with -6 V applied to the outer and $+3$ V applied to the inner endcap electrodes indicating an increase of cyclotron frequency with pressure. (b) Cyclotron frequency as a function of electron beam duration in the nested open cell indicating a linear dependence of cyclotron frequency on ion number. (c) Cyclotron frequency as a function of emission current in the nested open cell, also indicating a linear dependence of cyclotron frequency on ion number. (d) Plot of cyclotron frequency for benzene with increasing delay time in the nested open cell indicating that with time, coulomb repulsion opposes further reduction in axial extent of the ion cloud. (e) Comparison plot of cyclotron frequency as a function of electron beam duration in the closed cubic cell indicating an approximate linear reduction in cyclotron frequency as a function of ion number.

lizing portions of the trapping well. As a result of increased axial extent of the ion cloud due to coulomb repulsion and by the presence of negative charges in the outer trapping wells, this stabilizing feature of the open cell is maximized in experiments with nested traps that yield cyclotron frequency shifts 300 Hz higher than the unperturbed cyclotron frequency.

Acknowledgements

This work was supported by the Welch Foundation (F-1138), the National Institutes of Health, the Texas Advanced Research Program, and the National Science Foundation (CHE9013384 and CHE9057097).

References

- [1] M.B. Comisarow, A.G. Marshall, *Chem. Phys. Lett.* 25 (1974) 282.
- [2] R.C. Dunbar, *Int. J. Mass Spectrom. Ion Processes* 56 (1984) 1.
- [3] M.A. May, P.B. Grosshans, A.G. Marshall, *Int. J. Mass Spectrom. Ion Processes* 120 (1992) 193.
- [4] A.G. Marshall, F. Verdun, *Fourier Transforms in NMR, Optical and Mass Spectrometry*, Elsevier, Amsterdam, 1990.
- [5] G. Bollen, R.B. Moore, G. Savard, H. Stolzenberg, *J. Appl. Phys.* 68 (1990) 4355.
- [6] V.H. Vartanian, D.A. Laude, *Anal. Chem.* 68 (1996) 1321.
- [7] D.A. Dahl, SIMION 3D Version 6.0, Idaho National Engineering Laboratory, INEL-95/0403 Idaho Falls, ID, August, 1995.
- [8] J. Byrne, P.S. Farago, *Proc. Phys. Soc.* 86 (1965) 801.
- [9] J.H. Malmberg, J.S. deGrassie, *Phys. Rev. Lett.* 35 (1975) 577.
- [10] J.S. deGrassie, J.H. Malmberg, *Phys. Rev. Lett.* 39 (1977) 1077.
- [11] J.S. deGrassie, J.H. Malmberg, *Phys. Fluids* 23 (1980) 63.
- [12] G. Gabrielse, F.C. Mackintosh, *Int. J. Mass Spectrom. Ion Processes* 57 (1984) 1.
- [13] G. Gabrielse, X. Fei, K. Helmersson, S.L. Rolston, R. Tjoelker, T.A. Trainor, *Phys. Rev. Lett.* 57 (1986) 2504.
- [14] L.S. Brown, G. Gabrielse, *Rev. Mod. Phys.* 58 (1986) 233.
- [15] J. Tan, G. Gabrielse, *Appl. Phys. Lett.* 55 (1989) 2144.
- [16] G. Gabrielse, L. Haarsma, S.L. Rolston, *Int. J. Mass Spectrom. Ion Processes* 88 (1989) 319.
- [17] X. Fei, R. Davisson, G. Gabrielse, *Rev. Sci. Instrum.* 58 (1987) 2197.
- [18] W. Jhe, D. Phillips, L. Haarsma, J. Tan, G. Gabrielse, *Phys. Scripta* 46 (1992) 264.
- [19] S.C. Beu, D.A. Laude Jr., *Int. J. Mass Spectrom. Ion Processes* 112 (1992) 215.
- [20] V.L. Campbell, G. Ziqiang, V.H. Vartanian, D.A. Laude, *Anal. Chem.* 67 (1995) 420.
- [21] D.J. Griffiths, *Introduction to Electrodynamics*, 2nd ed., Prentice Hall, Englewood Cliffs, NJ, 1989.
- [22] S.A. McLuckey, G.J. Van Berkel, D.E. Goeringer, G.L. Glish, *Anal. Chem.* 66 (1994) 689A.
- [23] S. Guan, A.G. Marshall, *J. Am. Soc. Mass Spectrom.* 7 (1996) 101.
- [24] F.G. Major, H.G. Dehmelt, *Phys. Rev.* 170 (1968) 91.
- [25] C.-S.O., H.A. Schuessler, *J. Appl. Phys.* 52 (1980) 2601.
- [26] G.-Z. Li, G. Werth, *Phys. Scr.* 46 (1992) 587.
- [27] D.L. Rempel, M.L. Gross, *J. Am. Soc. Mass Spectrom.* 3 (1992) 590.
- [28] D.J. Bate, K. Dholakia, R.C. Thompson, D.C. Wilson, *J. Mod. Opt.* 39 (1992) 305.
- [29] M.V. Gorshkov, S. Guan, A.G. Marshall, *Rapid Commun. Mass Spectrom.* 6 (1992) 166.
- [30] S.-P. Chen, M.B. Comisarow, *Rapid Commun. Mass Spectrom.* 5 (1991) 450.
- [31] S.-P. Chen, M.B. Comisarow, *Rapid Commun. Mass Spectrom.* 6 (1992) 1.
- [32] F.H. Laukien, *Int. J. Mass Spectrom. Ion Processes* 73 (1986) 81.
- [33] M.B. Comisarow, in H. Hartmann, K.-P. Wanczek (Eds.), *Lecture Notes in Chemistry: Ion Cyclotron Resonance Mass Spectrometry*, Springer-Verlag, Berlin, 1978, p. 136.
- [34] M.B. Comisarow, *Adv. Mass. Spectrom.* 7 (1978) 1042.
- [35] J.S. Anderson, D.A. Laude, *Int. J. Mass Spectrom. Ion Processes* 157/158 (1996) 163.
- [36] C.L. Hendrickson, J.J. Drader, D.A. Laude Jr., S. Guan, A.G. Marshall, *Rapid Commun. Mass Spectrom.* 10 (1996) 1829.
- [37] V.H. Vartanian, D.A. Laude, *J. Am. Soc. Mass Spectrom.* 6 (1995) 812.
- [38] G. Gabrielse, S.L. Rolston, L. Haarsma, W. Kells, *Phys. Lett. A* 129 (1988) 38.
- [39] Y. Wang, K.-P. Wanczek, *Rev. Sci. Instrum.* 64 (1993) 883.
- [40] V.H. Vartanian, D.A. Laude, *Org. Mass Spectrom.* 29 (1994) 692.

- [41] D.S. Hall, G. Gabrielse, *Phys. Rev. Lett.* 77 (1996) 1962.
- [42] D.A. Laude Jr., S.C. Beu, *Anal. Chem.* 61 (1989) 2422.
- [43] J.D. Hogan, D.A. Laude Jr., *Anal. Chem.* 62 (1990) 530.
- [44] J.B. Jeffries, S.E. Barlow, G.H. Dunn, *Int. J. Mass Spectrom. Ion Processes* 54 (1983) 169.
- [45] V.H. Vartanian, D.A. Laude, unpublished results.
- [46] W. Quint, R. Kaiser, D. Hall, G. Gabrielse, *Hyperfine Interact.* 76 (1993) 181.
- [47] V.H. Vartanian, F. Hadjarab, D.A. Laude, *Int. J. Mass Spectrom. Ion Processes* 151 (1995) 175.
- [48] M. Wang, A.G. Marshall, *Anal. Chem.* 61 (1989) 1288.
- [49] E.R. Williams, K.D. Henry, F.W. McLafferty, *J. Am. Chem. Soc.* 112 (1990) 6157.
- [50] Z. Guan, S.A. Hofstadler, D.A. Laude Jr., *Anal. Chem.* 65 (1993) 1588.
- [51] J.P. Speir, G.S. Gorman, C.C. Pitsenberger, C.A. Turner, P.P. Wang, I.J. Amster, *Anal. Chem.* 65 (1993) 1746.
- [52] F.F. Chen, *Plasma Physics and Controlled Fusion*, 2nd ed., Plenum Press, New York, 1984, Chap. 5.
- [53] J.D. Williams, R.G. Cooks, *Rapid Commun. Mass Spectrom.* 7 (1993) 380.
- [54] E.A. Cornell, K.R. Boyce, D.L.K. Fyngenson, D.E. Pritchard, *Phys. Rev. A* 45 (1992) 3049.
- [55] M.A. Levine, R.E. Marrs, J.R. Henderson, D.A. Knapp, M.B. Schneider, *Phys. Scr.* T22 (1988) 157.
- [56] R. Becker, M. Kleinod, *Rev. Sci. Instrum.* 65 (1994) 1063.